RESEARCH FRONT

CSIRO PUBLISHING

Aust. J. Chem. **2014**, *67*, 1021–1029
http://dx.doi.org/10.1071/CH14134

Full Paper

Synthesis and Structural Characterization of a Series of Group 11 2,2-Dialkyl-1,3-dicyclohexylguanidinate Complexes

Sonya K. Adas,[A] *Jesus A. Ocana,*[A] *and Scott D. Bunge*[A,B]

[A]Kent State University, Department of Chemistry and Biochemistry,
Kent OH 44242, USA.
[B]Corresponding author. Email: sbunge@kent.edu

The addition of either lithium dimethylamide or lithium diethylamide to a tetrahydrofuran (THF) solution of 1,3-dicyclohexylcarbodiimide yielded THF adducts of lithium 2,2-dimethyl-1,3-dicyclohexylguandidinate (**1**) and lithium 2,2-diethyl-1,3-dicyclohexylguandidinate (**2**), respectively. One equivalent of either **1** or **2** was subsequently reacted with one equivalent of Group 11 halide (CuCl, AgBr, and AuCl) to generate oligonuclear complexes with the general formula $\{M[CyNC(NR_2)NCy]\}_n$ where M, R, and *n* are respectively Cu, CH_3, 2 (**3**); Cu, CH_2CH_3, 2 (**4**); Ag, CH_3, 3 (**5**); Ag, CH_2CH_3, 3 (**6**); Au, CH_3, 2 (**7**); and Au, CH_2CH_3, 2 (**8**). Compounds **1**–**8** were characterized by single-crystal X-ray diffraction. The bulk powders for all complexes were found to be in agreement with the crystal structures based on elemental analyses, Fourier transform infrared spectroscopy, and ^{1}H, ^{13}C, and ^{7}Li NMR studies. The unique structural aspects of this family of Group 11 complexes are highlighted.

Manuscript received: 11 March 2014.
Manuscript accepted: 16 April 2014.

Introduction

The use of the mono-anionic guanidinate ligand set has had a renaissance in the field of inorganic chemistry.[1–15] Guanidinates have developed into a versatile class of both *N*-donor and *N,N′*-donor ligands owing to the zwitterionic resonance of the ‘CN_3’ core. The dynamic resonance of the guanidinate anion facilitates delocalization of the negative charge on the coordinating N atom.[16] This resonance, coupled with steric and electronic tuning of the substituents, imparts the versatility necessary to readily coordinate hard and soft Lewis acids.[9–12] This degree of electronic stabilization is not obtained by using classic amido ligands such as NPh_2, NEt_2, and NMe_2.[17]

Owing to the unique nature of these ligands, multinuclear Group 11 guanidinate compounds have become well represented in the literature. These complexes have been studied for their potential to have closed shell d^{10}–d^{10} metal interactions, as reagents for atomic layer deposition, and for their luminescent properties.[18–24]

One of the underlying themes of our research has involved the development of 1,1,3,3-tetraalkylguanidinate (TAG) ligands (L^3, Fig. 1).[25–31] Our focus has been to use the N-donor to generate well-defined low-coordinate complexes. Using Group 11 metals, this ligand set resulted in the formation of novel hexanuclear, $[Cu(\mu\text{-TAG})]_6$ and tetranuclear $\{M_2(\mu\text{-TAG})[\mu\text{-N}(SiMe_3)_2]\}_2$ (M = Cu, Ag, and Au) structural motifs. Herein, we describe an extension of this work to the synthesis and characterization of Li, Cu, Ag, and Au complexes containing the 1,3-dicyclohexyl-2,2-dialkylguanidinate ligand $CyNC(NR_2)NCy$ (L^1, Fig. 1). Compounds **1**–**8** were characterized by single-crystal X-ray diffraction. The bulk powders for all complexes were in agreement with the crystal structures based on elemental analyses, Fourier transform infrared (FTIR) spectroscopy, and ^{1}H and ^{13}C NMR studies.

Experimental

Materials and Physical Measurements

All syntheses were handled with rigorous exclusion of air and water using standard glove box techniques. All anhydrous solvents were stored under argon and used as received in sure seal bottles. The following chemicals were used as received from commercial suppliers: lithium dimethylamide, lithium diethylamide, CuCl, AgBr, AuCl, and 1,2-dicyclohexylcarbodiimide. CuCl was purchased from a commercial supplier and purified using standard methods before use. $\{Cu[CyNC(NMe_2)NCy]\}_2$ (**3**) was synthesized according to a modified literature procedure.[32] FTIR data were obtained on a Bruker Tensor 27 spectrometer using KBr under an atmosphere of flowing nitrogen. Melting points of the samples were determined in sealed capillary tubes under an atmosphere of argon using an Electrothermal Mel-Temp apparatus and are uncorrected. Elemental analysis was performed on a Perkin–Elmer 2400 Series 2 CHN-S/O Elemental Analyzer. All NMR samples were prepared from dried crystalline materials that were handled and stored under an argon atmosphere and re-dissolved in [D8]toluene or [D6]benzene. All solution spectra were obtained on a Bruker DRX 400 spectrometer at 400.1, 155.5, and 100.6 MHz for ^{1}H, ^{7}Li, and ^{13}C experiments, respectively.

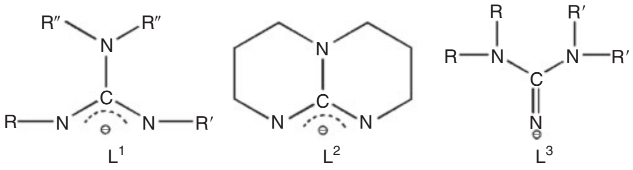

Fig. 1. Structures of mono-anionic guanidinate ligands. R = silyl; R′ = alkyl; R″ = aryl.

*{Li[CyNC(NMe$_2$)NCy](THF)}$_2$ (**1**)*

A 5 mL THF solution of 1,2-dicyclohexylcarbodiimide (0.36 g, 1.7 mmol) was added dropwise to a 10 mL THF solution of LiN(CH$_3$)$_2$ (0.088 g, 1.7 mmol). The reaction was stirred for 1 h. The reaction yielded a pale yellow solution, which was concentrated. The solution yielded colourless crystals at −35°C (0.41 g, 1.2 mmol, 72 %), mp 108°C. ν_{max} (KBr)/cm^{-1} 2979 (s), 2923 (s), 2848 (s), 2778 (m), 1637 (m), 1505 (s), 1446 (s), 1355 (s), 1312 (m), 1274 (w), 1251 (m), 1235 (m), 1180 (w), 1156 (m), 1121 (m), 1107 (m), 1061 (s), 1027 (w), 1002 (m), 916 (m), 902 (m), 888 (m), 843 (w), 804 (w), 782 (w), 764 (w), 675 (w), 629 (w), 546 (w), 499 (w), 462 (w), 427 (w). δ_H ([D6]benzene) 3.58 (THF), 3.41 (2H, m, NC*H*), 2.74 (6H, s, N(C*H*$_3$)$_2$), 2.20–1.20 (20H, m, Cy), 1.49 (THF). δ_C ([D6]benzene) 166.1 (NC*N*$_2$), 68.2 (N(*C*H$_3$)$_2$), 66.3 (THF), 55.2, 44.3, 37.7, 27.6 (Cy), 26.3 (THF). δ_{Li} ([D6]benzene) 2.1. Anal. Calc. for $C_{38}H_{72}Li_2N_6O_2$: C 69.27, H 11.01, N 12.75. Found: C 68.32, H 10.26, N 14.96 %.

*{Li[CyNC(NEt$_2$)NCy](THF)}$_2$·2(THF) (**2**)*

A 5 mL THF solution of dicyclohexylcarbodiimide (1.0 g, 5.0 mmol) was added dropwise to a 10 mL THF solution of LiN (CH$_2$CH$_3$)$_2$ (1.4 g, 5.0 mmol). The reaction was stirred for 1 h. The reaction yielded a pale yellow solution, which was centrifuged (1000 *g*, 25°C, 5 min) then concentrated. The solution yielded colourless crystals at −35°C (1.24 g, 4.3 mmol, 87 %), mp 68°C. ν_{max} (KBr)/cm^{-1} 2926 (s), 2852 (s), 2721 (s), 2665 (w), 2360 (w), 1636 (s), 1506 (s), 1449 (s), 1365 (s), 1339 (s), 1286 (m), 1257 (m), 1239 (m), 1211 (m), 1181 (w), 1143 (m), 1121 (w), 1071 (s), 1032 (w), 987 (w), 901 (w), 888 (w). δ_H ([D6]benzene) 3.61 (2H, m, NC*H*$_2$CH$_3$)$_2$), 3.59 (THF), 3.26–3.17 (4H, q, N(C*H*$_2$CH$_3$)$_2$), 3.13–3.105 (2H, m, NC*H*), 1.93–1.34 (20H, m, Cy), 1.71 (THF), 1.13–1.09 (6H, t, N(CH$_2$C*H*$_3$)$_2$). δ_C ([D8]benzene) 157.7 (NC*N*), 68.2 (N(*C*H$_2$CH$_3$)$_2$), 53.9, 43.6, 36.2, 35.2, 26.9, 26.3, 26.1 (Cy), 25.8 (THF), 13.3, 12.9 (N(CH$_2$*C*H$_3$)$_2$). δ_{Li} ([D6]benzene) 2.1. Anal. Calc. for $C_{42}H_{80}Li_2N_6O_2$: C 70.05, H 11.28, N 11.75. Found: C 69.76, H 11.24, N 12.75 %.

*{Cu[CyNC(NMe$_2$)NCy]}$_2$ (**3**)*

A 5 mL THF solution of 1,2-dicyclohexylcarbodiimide (1.0 g, 5.0 mmol) was added dropwise to a 10 mL THF solution of LiN(CH$_3$)$_2$ (0.26 g, 5.0 mmol). CuCl (0.50 g, 5.0 mmol) was then added to the mixture and the reaction was stirred for 1 h with the exclusion of light. The solution generated an off-white precipitate as the desired product. The powder was re-dissolved in toluene and crystallized at −35°C to give the final product (0.50 g, 1.6 mmol, 32 %). ν_{max} (KBr)/cm^{-1} 3001 (w), 2921 (s), 2848 (s), 2790 (m), 1504 (s), 1470 (s), 1387 (s), 1356 (m), 1341 (m), 1272 (w), 1252 (m), 1228 (m), 1181 (w), 1128 (m), 1110 (w), 1174 (m), 1118 (m), 964 (w), 920 (w), 907 (w), 887 (m), 844 (w), 814 (w), 790 (w), 740 (w), 710 (w), 656 (w), 509 (w), 458 (w). δ_H ([D8]toluene) 2.98 (2H, m, NC*H*), 2.62 (6H, s, N (C*H*$_3$)$_2$), 2.04–1.00 (20H, m, Cy). δ_C ([D8]toluene) 172.2 (NC*N*), 68.5 (N(*C*H$_3$)$_2$), 58.1, 41.7, 39.8, 29.3 (Cy). Anal. Calc. for $C_{30}H_{56}Cu_2N_6$: C 57.39, H 8.99, N 13.38. Found: C 57.52, H 9.27, N 13.39 %.

*{Cu[CyNC(NEt$_2$)NCy]}$_2$ (**4**)*

A 5 mL THF solution of 1,2-dicyclohexylcarbodiimide (1.04 g, 5.0 mmol) was added dropwise to a 10 mL THF solution of LiN(CH$_2$CH$_3$)$_2$ (0.26 g, 5.0 mmol). CuCl (0.50 g, 5.0 mmol) was ground to a fine powder then added dry to the mixture and the reaction was stirred for 1 h with the exclusion of light. The reaction generated a dark orange solution that was centrifuged (1000 *g*, 25°C, 5 min) then concentrated. The solution yielded colourless crystals at −35°C (0.41 g, 0.60 mmol, 24 %), mp 129°C (dec.). ν_{max} (KBr)/cm^{-1} 2927 (s), 2852 (s), 1536 (s), 1449 (m), 1400 (w), 1364 (w), 1340 (w), 1282 (w), 1143 (w), 1089 (w), 1030 (w), 889 (w), 804 (w), 616 (w), 446 (m). δ_H ([D6] benzene) 3.60−3.57 (4H, m, N(C*H*$_2$C*H*$_3$)$_2$), 3.25–3.09 (2H, m, NC*H*), 1.96–1.34 (20H, m, Cy), 1.23–1.01 (6H, t, *J* 8.8, N (CH$_2$C*H*$_3$)$_2$). δ_C ([D6]benzene) 172.6 (NC*N*), 67.5 (N (*C*H$_2$CH$_3$)$_2$), 58.3, 52.6, 45.6, 41.7, 39.8, 37.5, 35.5, 29.3, 27.7, 27.1 (Cy), 13.5, 12.1 (N(CH$_2$*C*H$_3$)$_2$). Anal. Calc. for $C_{34}H_{64}Cu_2N_6$: C 59.70, H 9.43, N 12.29. Found: C 60.22, H 10.13, N 13.45 %.

*{Ag[CyNC(NMe$_2$)NCy]}$_3$ (**5**)*

A 5 mL THF solution of 1,2-dicyclohexylcarbodiimide (1.0 g, 5.0 mmol) was added dropwise to a 10 mL THF solution of LiN(CH$_3$)$_2$ (0.26 g, 5.0 mmol). AgBr (0.95 g, 5.0 mmol) was then added to the mixture and the reaction was stirred for 1 h in the exclusion of light. The solution generated an off-white precipitate as the desired product. The powder was re-dissolved in toluene and crystallized at −35°C to generate the final product (0.32 g, 0.90 mmol, 18 %), mp 110°C (dec.). ν_{max} (KBr)/cm^{-1} 2985 (w), 2921 (s), 2849 (s), 2790 (m), 2664 (w), 1496 (s), 1445 (s), 1387 (s), 1355 (m), 1342 (m), 1315 (w), 1277 (w), 1255 (m), 1230 (m), 1182 (w), 1150 (w), 1125 (m), 1088 (w), 1068 (m), 1016 (m), 961 (w), 920 (w), 906 (w), 887 (m), 846 (w), 810 (w), 784 (w), 699 (w), 637 (w), 551 (w), 454 (w), 429 (w). δ_H ([D8] toluene) 3.12 (2H, m, NC*H*), 2.694 (6H, s, N(C*H*$_3$)$_2$), 2.0–1.0 (20H, m, Cy). δ_C ([D8]toluene) 169.6 (NC*N*), 67.9 (N(*C*H$_3$)$_2$), 57.6, 41.1, 39.5, 26.8 (Cy). Anal. Calc. for $C_{45}H_{84}Ag_3N_9$: C 50.29, H 7.88, N 11.73. Found: C 47.96, H 7.61, N 10.86 %.

*{Ag[CyNC(NEt$_2$)NCy]}$_3$·(THF) (**6**)*

A 5 mL THF solution of 1,2-dicyclohexylcarbodiimide (1.0 g, 5.0 mmol) was added dropwise to a 10 mL THF solution of LiN(CH$_2$CH$_3$)$_2$ (0.39 g, 5.0 mmol). AgBr (0.95 g, 5.0 mmol) was ground to a fine powder then added dry to the mixture and the reaction was stirred for 1 h in the exclusion of light. The reaction generated a dark grey solution. THF was removed to yield a white powder. The powder was re-dissolved in toluene and crystallized at −35°C to generate the final product (0.48 g, 0.41 mmol, 8.3 %). ν_{max} (KBr)/cm^{-1} 2925 (s), 2851 (s), 2721 (m), 1635 (s), 1505 (s), 1449 (m), 1359 (m), 1339 (m), 1288 (m), 1239 (w), 1211 (w), 1143 (w), 1122 (w), 1072 (m), 998 (w), 888 (m), 804 (w), 630 (w), 498 (w), 472 (w). δ_H ([D6]benzene) 3.62–3.55 (4H, m, N(C*H*$_2$CH$_3$)$_2$), 3.24–3.10 (2H, m, NC*H*), 2.11–1.39 (20H, m, Cy), 1.17–1.13 (6H, t, *J* 7.05, N(CH$_2$C*H*$_3$)$_2$). δ_C ([D6] benzene) 170.4 (NC*N*), 68.2 (N(*C*H$_2$CH$_3$)$_2$), 57.4, 53.9, 44.52, 43.6, 37.7, 36.2, 35.7, 27.7, 27.0, 26.1 (Cy), 14.8, 13.3

($N(CH_2CH_3)_2$). Anal. Calc. for $C_{51}H_{96}CAg_3N_9$: C 52.85, H 8.35, N 10.88. Found: C 52.08, H 8.66, N 10.89 %.

*{Au[CyNC(NMe₂)NCy]}₂ (**7**)*

A 5 mL THF solution of 1,2-dicyclohexylcarbodiimide (1.0 g, 5.0 mmol) was added dropwise to a 10 mL THF solution of $LiN(CH_3)_2$ (0.26 g, 5.0 mmol). AuCl (0.40 g, 1.7 mmol) was then added to the mixture and the reaction was stirred for 1 h with the exclusion of light. The solution generated a dark precipitate, which was centrifuged (1000 *g*, 25°C, 5 min) off. The remaining solution was allowed to crystallize by slow evaporation to generate the final product (0.34 g, 0.70 mmol, 44 %), mp 63°C (dec.). ν_{max} (KBr)/cm^{-1} 2999 (w), 2924 (s), 2849 (s), 2790 (m), 1635 (s), 1579 (s), 1505 (s), 1465 (s), 1386 (s), 1358(m), 1342 (m), 1247 (s), 1225 (m), 1183 (w), 1131 (m), 1105 (w), 1072 (w), 1023 (w), 978 (w), 956 (w), 921 (w), 910 (w), 889 (m), 846 (w), 810 (w), 793 (w), 736 (w), 711 (w), 696 (w), 648 (w), 627 (w), 590 (w), 560 (w), 509 (w), 461 (w), 436 (w). δ_H ([D8]toluene) 3.25 (2H, m, NC*H*), 2.70, 2.50 (6 H, d, $N(CH_3)_2$), 1.9–1.0 (20H, m, Cy). δ_C ([D8]toluene) 171.4 (N*C*N), 68.2 ($N(CH_3)_2$), 59.7, 41.4, 40.3, 39.0 (Cy). Anal. Calc. for $C_{30}H_{56}Au_2N_6$: C 40.18, H 6.52, N 9.37. Found: C 41.29, H 6.90, N 9.32 %.

*{Au[CyNC(NEt₂)NCy]}₂·(THF) (**8**)*

Compound **2** (1.2 g, 1.7 mmol) was dissolved in 10 mL of THF and cooled to −34°C. AuCl (0.40 g, 1.7 mmol) was then added and the reaction was stirred for 1 h with the exclusion of light. The solution generated a small amount of dark precipitate, which was centrifuged (1000 *g*, 25°C, 5 min) off. The remaining solution was re-crystallized by slow evaporation to generate the final product (0.57 g, 0.60 mmol, 35 %), mp 78°C (dec.). ν_{max} (KBr)/cm^{-1} 2927 (s), 2852 (m), 2720 (m), 1636 (s), 1577 (w), 1449 (m), 1400 (m), 1363 (s), 1340 (m), 1307 (w), 1282 (s), 1258 (w), 1240 (w), 1207 (w), 1143 (w), 1090 (w), 1072 (w), 1045 (w), 889 (w). δ_H ([D6]benzene) 3.70–3.25 (6H, m, $N(CH_2CH_3)_2$ and NC*H*), 1.25–1.22 (6H, t, *J* 7.0, $N(CH_2CH_3)_2$), 2.02–0.97 (20H, m, Cy). δ_C ([D6]benzene) 153.7 (N*C*N), 68.2 ($N(CH_2CH_3)_2$), 56.7, 53.9, 43.6, 36.3, 35.3, 34.8, 26.9, 26.4, 26.1 (Cy), 13.3 ($N(CH_2CH_3)_2$). Anal. Calc. for $C_{34}H_{64}Au_2N_6$: C 42.95, H 6.78, N 8.84. Found: C 42.17, H 6.65, N 7.92 %.

X-Ray Structural Studies

X-ray crystallography was performed by mounting each colourless crystal sample **1**–**8** onto a thin glass fibre from a pool of Fluorolube™ and immediately placing it under a liquid N_2-cooled N_2 stream on a Bruker AXS diffractometer. The radiation used was graphite monochromatized Mo$_{K\alpha}$ (λ 0.7107 Å). The lattice parameters were optimized from a least-squares calculation on carefully centred reflections. Lattice determination, data collection, structure refinement, scaling, and data reduction were carried out using *APEX2* (version 2014–1.1) software package.

Each structure was solved using direct methods. This procedure yielded Ag, Au, Cu, or Li atom along with several O, N, and C atoms. Subsequent Fourier synthesis yielded the remaining atom positions. The hydrogen atoms were fixed in positions of ideal geometry and refined using the *XSHELL* software. These hydrogen atoms had their isotropic temperature factors fixed at either 1.2 or 1.5 times of the equivalent isotropic U of the C atoms to which they were bonded. The final refinement of each compound included anisotropic thermal parameters on all non-hydrogen atoms.

Computational Details

Becke's gradient-corrected exchange and LYP correlation functional and its hybrid which form the B3 LYP level of theory[33,34] was employed along with the Wachters[35] and Hay[36] LANL2DZ basis set for molecular orbital and natural bond orbital (NBO)[37] calculations. All molecular orbital calculations were done with the *Spartan'04* package[38] and the coordinates for the atoms in each structure were taken from the crystallographic data. NBO analysis was conducted using the *Gaussian 98* package.[39,40]

Results and Discussion

Synthesis

Lithium 2,2-dialkyl-1,3-dicyclohexylguanidinate may be straightforwardly generated via the reaction between lithium dialkylamide and 1,2-dicyclohexylcarbodiimide. This ligand has been successfully employed to facilitate the isolation of monomeric early transition metal complexes e.g. $\{[\sigma:\eta^1:\eta^5\text{-}(OCH_2)(Me_2NCH_2)C_2B_9H_9]Ti[\eta^3\text{-}CyNC(NMe_2)NCy]\}$, {Ta $(NMe_2)_4$[CyNC(NMe$_2$)NCy]}, and Zr {Zr[CyNC(N^{i}Pr$_2$)NCy] Cl$_3$}.[41–50] Herein, we report the use of this approach to cleanly generate {Li[CyNC(NR$_2$)NCy](THF)}$_2$ where NR$_2$ = NMe$_2$ (**1**) and NEt$_2$ (**2**) (Scheme 1). Compounds **1** and **2** were subsequently reacted with MX (MX = CuCl, AgBr, and AuCl) to form the corresponding guanidinate complex {M[CyNC(NR$_2$)NCy]}$_n$ where M, R, and *n* are respectively Cu, CH_3, 2 (**3**); Cu, CH_2CH_3, 2 (**4**); Ag, CH_3, 3 (**5**); Ag, CH_2CH_3, 3 (**6**); Au, CH_3, 2 (**7**); and Au, CH_2CH_3, 2 (**8**). The synthesis of compounds **3**–**8** is shown in

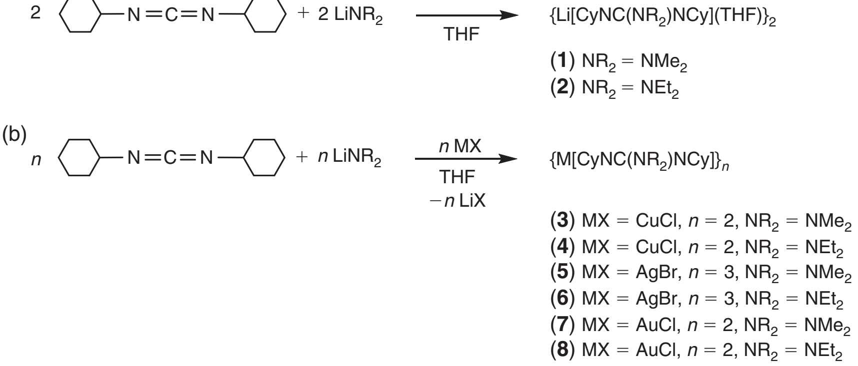

Scheme 1. Synthesis of (a) **1**–**2** and (b) **2**–**4**.

Scheme 1. Owing to the photosensitivity of the Group 11 complexes, the reactions are shielded from light throughout the course of the synthesis. In each of these reactions, reduction to elemental metal is observed and the insoluble precipitate is removed from solution via centrifugation before concentration. The reaction mixture is concentrated and cooled to −35°C to facilitate isolation of **1**–**8** as colourless crystals. For elemental analysis, re-crystallization was additionally performed by re-dissolving the isolated solid in a THF/hexanes (1 : 1) mixture and then cooling the sample to −35°C for 24 h. Photosensitivity precluded obtaining satisfactory elemental analysis for several samples. Dry crystals of **1**–**8** are stable under argon at −35°C in the absence of light for several months.

Spectroscopic Studies

Crystals of **1**–**8** were dried under vacuum to obtain a bulk powder for use in subsequent studies. FTIR spectroscopic studies revealed the absence of a characteristic n=C=N stretch (2117 $\mathrm{cm^{-1}}$) and the presence of a C=N stretch typical of $\mathrm{L^1}$ guanidinates (1496 to 1474 $\mathrm{cm^{-1}}$).[51] Compounds **1**–**8** were moderately soluble in [D6]benzene and [D8]toluene, and revealed expected resonances in the ^{1}H and ^{13}C NMR spectra. In particular, all of the spectra show low-field resonances in the ^{13}C NMR analysis that are characteristic of guanidinates (~160 ppm). Inherent asymmetry within the [CyNC(NEt$_2$)NCy] ligated complexes (**2**, **4**, **6**, and **8**) results in multiple resonances in the ^{13}C NMR spectra assignable to the cyclohexyl and ethyl substituents. Additionally, the ^{7}Li NMR spectra for compounds **1** and **2** reveal a single peak at 2.1 ppm.

Structural Description

All eight complexes were characterized by X-ray crystallography. Thermal ellipsoid plots of **1**–**8** are shown in Figs 2–5 and Figs S1–S4 (Supplementary Material). The data collection parameters are presented in Tables 1 and 2, and selected inter-atomic distances and angles are included with the plots in Table 3. Structural descriptions of the complexes are presented in the

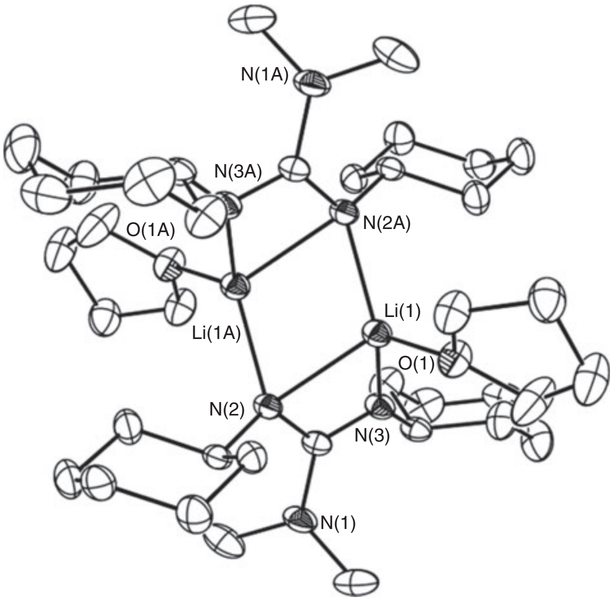

Fig. 2. Thermal ellipsoid plot of **1**. Ellipsoids are drawn at the 30 % level. H atoms have been omitted for clarity. The additional 'A' letters in the atom labels indicate that these atoms are at (–*x* + 1, –*y*, –*z*). Selected inter-atomic distances (Å) and angles (°): Li(1)–O(1) 1.942(3), Li(1)–N(3) 1.991(3), Li(1)–N(2A) 2.066(3), Li(1)–N(2) 2.184(3) Å, O(1)–Li(1)–N(3) 115.74(15), O(1)–Li(1)–N(2A) 110.04(14), N(3)–Li(1)–N(2A) 129.52(16), O(1)–Li(1)–N(2) 118.82(15), N(3)–Li(1)–N(2) 66.14(10), N(2A)–Li(1)–N(2) 108.74(13)°.

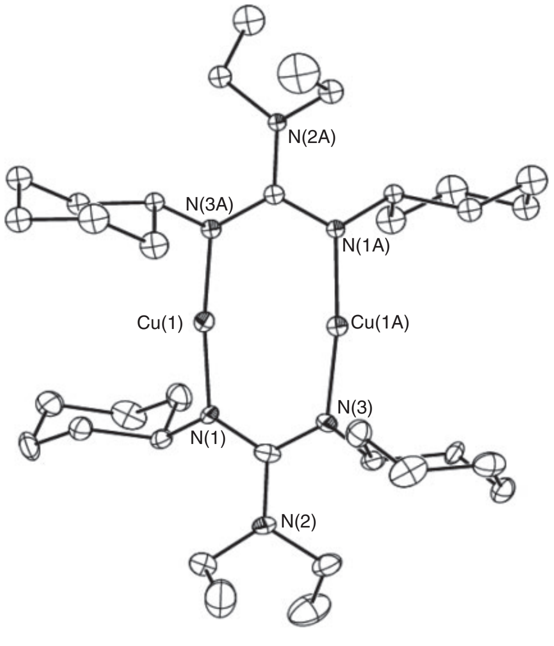

Fig. 3. Thermal ellipsoid plot of **4**. Ellipsoids are drawn at the 30 % level. H atoms have been omitted for clarity. The additional 'A' letters in the atom labels indicate that these atoms are at (–*x* + 1, –*y*, –*z*). Selected inter-atomic distances (Å) and angles (°): Cu(1)–N(3A) 1.870(6), Cu(1)–N(1) 1.875(6), Cu(2)–N(3) 1.870(6), Cu(2)–N(1A) 1.875(6) Å, N(3A)–Cu(1)–N(1) 173.2(3), N(3)–Cu(2)–N(6) 173.2(3)°.

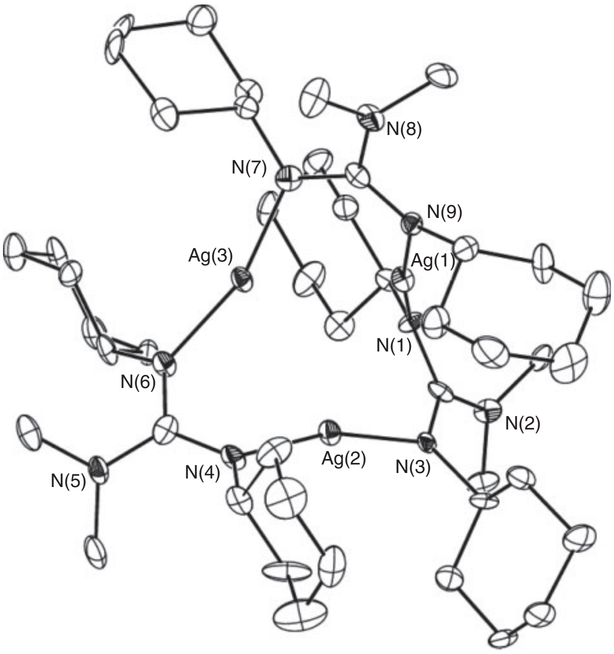

Fig. 4. Thermal ellipsoid plot of **5**. Ellipsoids are drawn at the 30 % level. H atoms have been omitted for clarity. Selected inter-atomic distances (Å) and angles (°): Ag(1)–N(1) 2.096(8), Ag(1)–N(9) 2.109(9), Ag(2)–N(4) 2.100(9), Ag(2)–N(3) 2.121(8), Ag(3)–N(6) 2.093(9), Ag(3)–N(7) 2.095(9) Å, N(1)–Ag(1)–N(9) 169.5(3), N(4)–Ag(2)–N(3) 163.2(3), N(6)–Ag(3)–N(7) 162.3(4)°.

following paragraphs. Owing to the similarity, when appropriate, a general description of the complexes is provided. Table 3 lists selected inter-atomic distance and angles for structurally characterized Group 11 L^1 and L^2 guanidinate complexes.

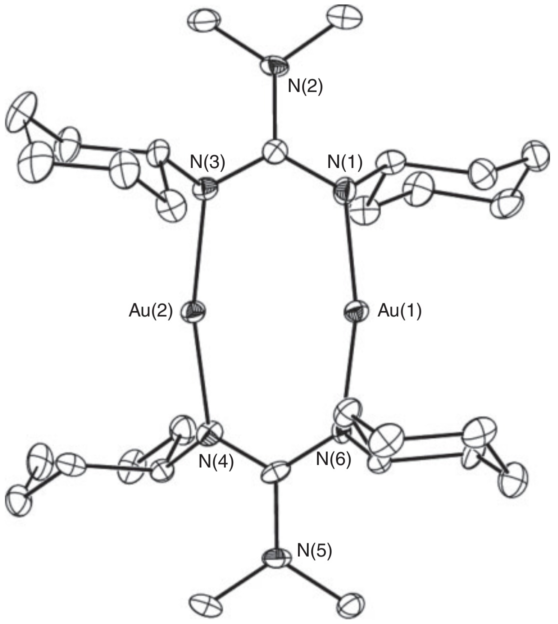

Fig. 5. Thermal ellipsoid plot of **7**. Ellipsoids are drawn at the 30 % level. H atoms have been omitted for clarity. Selected inter-atomic distances (Å) and angles (°): Au(1)–N(6) 2.025(9), Au(1)–N(1) 2.048(10), Au(2)–N(4) 2.028(9), Au(2)–N(3) 2.044(9) Å, N(6)–Au(1)–N(1) 167.7(3), N(4)–Au(2)–N(3) 166.8(4)°.

*{Li[CyNC(NMe$_2$)NCy](THF)}$_2$ (**1**) and {Li[CyNC(NEt$_2$)NCy](THF)}$_2$ (**2**)*

Thermal ellipsoid plots of **1** and **2** are given in Figs 2 and S1. Both **1** and **2** are centrosymmetric dimers that adopt a 'ladder' structure similar to that of previously reported solvated lithium dialkyl-1,3-dialkylguanidinate complexes i.e. {Li[^{i}PrNC(N^{i}Pr$_2$)N^{i}Pr](THF)}$_2$, {Li[CyNC(NCH$_2$CH$_2$CH$_2$CH$_2$)$_2$)NCy](THF)}$_2$, and {Li[CyNC(N^{i}Pr$_2$)NCy](Et$_2$O)}$_2$.[52–54] In **1** and **2**, each lithium metal has a coordination number of four where Li(1) is coordinated to one terminal THF molecule (Li(1)–O(1) 1.942(3) Å in **1** and 1.928(7) Å in **2**). Each Li is connected to an adjacent Li by two bridging N atoms (Li(1)–N(3) 1.991(3), Li(1)–N(2) 2.184(3) Å in **1** and Li(1)–N(2) 1.991(7), Li(1)–N(1) 2.282(8) Å in **2**). The Li coordination sphere is completed by further coordination to an additional N atom from the guanidinate (Li(1)–N(2A) 2.066(3) Å in **1** and Li(1)–N(1) 2.050(7) Å in **2**). The Li–O(THF) bond lengths are in agreement with the average value of 1.94(6) Å from the Cambridge Structural Database.[55,56] Li–N(3)–C(1)–N(2) in **1** and Li–N(2)–C(11)–N(1) in **2** form a nearly planar four-membered ring with maximum deviations of 0.131 Å and 0.122 Å, respectively, on either side of the planar central Li$_2$N$_2$ ring. These central and side planes form dihedral angles of 51.38° and 52.25° in **1** and **2**, respectively. Owing to the symmetry of the molecule, the planes of the guanidinate CN$_3$ structure are parallel and deviate by 0.278 Å and 0.374 Å. However, the CN$_3$ plane in **1** and **2** deviate only by 4.31° and 5.74°, respectively, from the base of the pyramidal structure. To quantify the four-coordinate geometry around the metal centre, the τ_4 parameter[57] was calculated from the two largest angles in **1** (N(3)–Li(1)–N(2A) 129.5° and N(2)–Li(1)–O(1) 118.8°) and **2** (N(2)–Li(1)–N(1A) 129.0° and N(1)–Li(1)–O(1) 118.8°). The geometry around the metal centre

Table 1. Data collection parameters for 1–4

	Compound			
	1	**2**	**3**	**4**
Chemical formula	$C_{38}H_{72}Li_2N_6O_2$	$C_{50}H_{96}Li_2N_6O_4$	$C_{30}H_{56}Cu_2N_6$	$C_{34}H_{64}Cu_2N_6$
Formula weight	658.9	859.20	658.9	683.99
T [K]	189(2)	189(2)	160(2)	180(2)
Space group	Monoclinic $P2(1)/c$	Monoclinic $P2(1)/c$	Triclinic $P\bar{1}$	Monoclinic $P2(1)/c$
Size [mm]	0.38 × 0.31 × 0.23	0.10 × 0.10 × 0.10	0.20 × 0.19 × 0.12	0.35 × 0.30 × 0.20
a [Å]	10.9032(16)	13.442(4)	10.4108(16)	13.397(13)
b [Å]	18.073(3)	18.884(6)	11.3907(15)	7.098(8)
c [Å]	10.6721(17)	11.606(4)	16.049(3)	22.211(18)
α [°]			97.117(3)	
β [°]	103.214(4)	113.617(4)	107.487(2)	119.27(5)
γ [°]			112.556(4)	
V [Å^3]	2047.2(5)	2699.4(15)	1613.4(4)	1842(3)
Z	2	4	2	2
D_c [Mg m^{-3}]	1.069	0.880	1.292	1.233
Reflections collected (unique)	16199 (3617)	18952 (4767)	13151 (5720)	14095 (3263)
GOF (parameters)	0.856 (219)	0.796 (237)	0.759 (347)	0.853 (192)
$\Delta\rho_{\max}$ [e Å^{-3}]	0.286	0.233	0.357	0.438
$T_{\min}/T_{\max}$	0.894/0.985	0.824/0.993	0.558/0.855	0.680/0.796
$\mu(\mathrm{Mo_{K\alpha}})$ [mm^{-1}]	0.065	0.053	1.346	1.184
R_1^{A} [%] (all data)	4.82 (6.66)	8.69 (22.95)	3.21 (4.54)	6.57 (17.40)
wR_2^{B} [%] (all data)	13.94 (15.94)	20.04 (25.11)	9.41 (10.86)	14.44 (21.06)

$^{\mathrm{A}}R_1 = \Sigma(||F_o| - |F_c||)/\Sigma|F_o| \times 100\,\%$.
$^{\mathrm{B}}wR_2 = [\Sigma w(F_o^2 - F_c^2)^2/\Sigma(w|F_o|^2)^2]^{1/2} \times 100\,\%$.

Table 2. Data collection parameters for 5–8

	Compound			
	5	**6**	**7**	**8**
Chemical formula	$C_{49}H_{92}Ag_3N_9O$	$C_{51}H_{96}Ag_3N_9$	$C_{30}H_{56}Au_2N_6$	$C_{38}H_{56}Au_2N_6O$
Formula weight	1146.92	1158.98	894.74	1022.94
T [K]	160(2)	189(2)	189(2)	189(2)
Space group	Monoclinic $P2(1)/n$	Triclinic $P\bar{1}$	Triclinic $P\bar{1}$	Tetragonal $P\bar{4}b2$
Size [mm]	0.29 × 0.15 × 0.12	0.30 × 0.20 × 0.20	0.20 × 0.19 × 0.14	0.10 × 0.08 × 0.05
a [Å]	13.663(8)	12.986(4)	10.4435(3)	16.622(2)
b [Å]	17.927(10)	14.266(4)	11.5080(3)	16.622(2)
c [Å]	22.310(13)	17.000(5)	16.0854(4)	7.6463(14)
α [°]		95.134(5)	97.535(2)	
β [°]	99.680(10)	95.318(4)	106.587(2)	
γ [°]		114.367(4)	112.530(2)	
V [Å^3]	5387(5)	2828.0(13)	1646.98(8)	2112.5(7)
Z	4	2	2	2
D_c [Mg m^{-3}]	1.414	1.363	1.804	1.608
Reflections collected (unique)	28356 (9505)	22579 (9993)	39364 (5838)	1947 (1569)
GOF (parameters)	0.946 (565)	0.903 (574)	0.846 (347)	0.992 (98)
$\Delta\rho_{max}$ [e Å^{-3}]	0.656	0.667	1.123	0.865
T_{min}/T_{max}	0.286/0.877	0.683/0.814	0.268/0.368	0.737/0.877
μ(Mo$_{K\alpha}$) [mm^{-1}]	1.122	1.068	8.925	6.971
R_1^A [%] (all data)	6.94 (18.60)	6.00 (11.68)	3.79 (7.49)	4.55 (6.58)
wR_2^B [%] (all data)	11.13 (15.17)	14.30 (18.58)	10.06 (13.51)	13.14 (14.26)

[A] $R_1 = \Sigma(||F_o| - |F_c||)/\Sigma|F_o| \times 100\,\%$.

[B] $wR_2 = [\Sigma w(F_o^2 - F_c^2)^2/\Sigma(w|F_o|^2)^2]^{1/2} \times 100\,\%$.

Table 3. Structurally characterized Group 11 L^1 and L^2 guanidinate complexes

	Complex			Reference
	M–N [Å]	M···M [Å]	N–M–N [°]	
Cu				
$\{Cu[^iPrNC(NMe_2)N^iPr]\}_2$	1.88	2.42	174.75	[61]
$\{Cu[^iPrNC(NH^iPr)N^iPr]\}_2$	1.88	2.43	173.71	[61]
$\{Cu[CyNC(NEt_2)NCy]\}_2$ (**4**)	1.87	2.43	173.23	A
$\{Cu[CyNC(NMe_2)NCy]\}_2$ (**3**)	1.88	2.44	170.33	A
$\{Cu\{CyNC(NMe_2)NCy]\}_2$	1.88	2.44	170.56	[32]
$[Cu_2(hpp)_2]$	1.86	2.45	175.98	[58]
$\{Cu[(C_6H_3{}^iPr_2\text{-}2,6)NC(NCy_2)N(C_6H_3{}^iPr_2\text{-}2,6)]\}_2$	1.90	2.40	176.8	[65]
Ag				
$[Ag_4(hpp)_4]$	2.08	2.86	172.1	[20]
$\{Ag[CyNC(NMe_2)NCy]\}_3$ (**5**)	2.10	3.04	165.0	A
$\{Ag[CyNC(NEt_2)NCy]\}_3$ (**6**)	2.10	3.04	164.9	A
Au				
$[Au_2(hpp)_2Cl_2]$	2.04	2.48	169.4	[20]
$\{Au[^iPrNC(NMe_2)N^iPr]\}_2$	2.04	2.66	170.7	[18]
$\{Au[CyNC(NEt_2)NCy]\}_2$ (**8**)	2.03	2.66	165.8	A
$\{Au[CyNC(NMe_2)NCy]\}_2$ (**7**)	2.04	2.67	166.3	A
$[Au_4(hpp)_4]$	2.02	2.92	173.7	[22]

[A] This work.

closely resembles a distorted trigonal pyramidal (C_{3v}) geometry with a τ_4 value[57] of 0.79 for both **1** and **2**.

$\{Cu[CyNC(NMe_2)NCy]\}_2$ (3) and $\{Cu[CyNC(NEt_2)NCy]\}_2$ (4)

Thermal ellipsoid plots of **4** and **3** are given in Figs 3 and S2, respectively. The structure of **3** has been previously reported and it is metrically similar to the previous data acquired (Table 3). In **3** and **4**, each complex contains two Cu atoms bridged by two guanidinate ligands in a μ, $\eta^1:\eta^1$-fashion. The average Cu–N distance is 1.877 Å in **3** and 1.872 Å in **4**, similar to that observed in analogous compounds copper guanidinates (Table 3).[18,58] Cu–Cu distances for **3** and **4** are 2.437 Å and 2.438 Å, respectively. These fall within the range of general Cu–Cu distances with bridging ligands, and are much shorter than the Cu–Cu distance in metallic copper.[59] The N–Cu–N angles in **3** and **4** are 170.33° and 173.23°, respectively, and deviate from linearity and analogous compounds in the literature.[18,60] This is attributed to the added steric strain from the cyclohexyl groups, generating a decrease in the Cu–Cu separation. Density functional theory (DFT) calculations are used to investigate any Cu–Cu interactions owing to this decrease in linearity and the short Cu–Cu distance.[60–62] Both **3** and **4** support the delocalization of the imine bond across the two coordinating nitrogen atoms, resulting in C–N distances ranging from 1.334 to 1.343 Å. This is further supported by the co-planarity of the N–C–N backbone, whereby in each case an angle close to 120° was observed. Torsion angles of 48.01° for **3** and 34.84° for **4** are observed for the plane of one N–C–N of the guanidinate to the plane of the other. The significant difference in the torsion angle may be attributed to steric repulsions between the ethyl groups and the peripheral cyclohexyl rings. The small values of these torsion angles is a further indication that electron delocalization is present within the guanidinate ligands.

*{Ag[CyNC(NMe$_2$)NCy]}$_3$ (**5**) and {Ag[CyNC(NEt$_2$)NCy]}$_3$ (**6**)*

Thermal ellipsoid plots of **5** and **6** are given in Figs 4 and S3, respectively. Each complex forms a trimeric cluster. In the structures, each guanidinate ligand bridges two silver atoms together in a $\eta^1:\eta^1$-fashion, enclosing three metal centres, similar to the silver amidinate trimer [Ag(*N*,*N'*-diisopropylacetamidinate)]$_3$[60] and the silver guanidinate trimer {Ag[^{i}PrNC(NMe$_2$)N^{i}Pr]}$_3$.[18] The centre of the structures consists of three Ag atoms that are arranged in a triangular fashion with Ag–Ag distances of 2.994, 2.940, and 3.177 Å in **5**, and 2.995, 2.988, and 3.172 Å in **6**, and Ag···Ag···Ag angles in the range of 57° to 65° in each complex. The cluster contains Ag–N bonds ranging from 2.093 to 2.120 Å in **5**, and from 2.075 to 2.108 Å in **6**. The smaller Ag–N distance in **6** is tentatively attributed to the increase in steric repulsions from the presence of the bulkier ethyl substituents. These angles and distances are in agreement with similar complexes in the literature.[18,60] Two ligands coordinate to each Ag metal centre in a linear fashion, with an average N–Ag–N bond angle of 165° in both **5** and **6**. The guanidinate ligands are twisted across the molecule owing to steric interactions. As such, the planes of each form 60, 67, and 85° angles to one another in **5**, and 68, 71, and 82° angles to one another in **6**. Also, the guanidinates produce 40, 48, and 49° torsion angles with respect to the plane of the Ag metal centres in **5**, and 40, 50, and 53° torsion angles in **6**.

*{Au[CyNC(NMe$_2$)NCy]}$_2$ (**7**) and {Au[CyNC(NMe$_2$)NCy]}$_2$ (**8**)*

Thermal ellipsoid plots of **7** and **8** are given in Figs 5 and S4, respectively. In each structure, the two Au atoms are bound by two guanidinate molecules. Each ligand contributes a coordinated nitrogen to each metal centre, where the average Au–N bond length is 2.03 Å. The Au metal centres both hold nearly linear coordination sites with angles of 167°. This conformation allows the Au metal centres to be separated by a distance of 2.6 Å. The cyclohexyl groups are staggered between the two ligands thus resulting in a torsion angle of 36.0°, where the distance between the two Au centres bisects this torsion angle. The plane of the amino substituent has a torsion angle of ~36.0° with respect to its corresponding guanidinate backbone. Each compound has metrical parameters similar to those of the previously reported {Au[^{i}PrNC(NMe$_2$)N^{i}Pr]}$_2$ (Table 3). A notable difference between **7** and **8** and the previous report is a slight decrease in the N–Au–N angle; attributable to an increase in steric congestion contributed by the cyclohexyl substituents relative to the isopropyl groups in the previous report.

Guanidinate Resonance

The resonance structure of the L^1 TAG anion facilitates delocalization of the negative charge on the N$_{\text{imino}}$ atom. A convenient method to assess the extent of delocalization within the '–*n*=C–N–' component of the guanidinate ligand is the via evaluation of the Δ_{CN} parameter: $\Delta_{CN} = d(\text{C–N}) - d(\text{C=N})$.[63] The Δ_{CN} values range from 0 Å in a fully delocalized system to up to ~0.10 Å in a fully localized system. The Δ_{CN} values for complexes **1**–**8** were calculated from crystallographic data: **1** (0.026 Å), **2** (0.055 Å), **3** (0.009 and 0 Å), **4** (0.003 Å), **5** (0.030, 0.024, and 0.012 Å), **6** (0.012, 0.004, and 0.001 Å), **7** (0.009 Å), and **8** (0 Å). From these values, it can be determined that a slight localization of charge exists within the amidine moiety for the Li complexes **1** and **2**, and in the trinuclear Ag complex **5**. For complexes **3**–**4** and **6**–**8**, there is significant delocalization across the N–C–N unit.

To further examine the potential zwitterionic resonance of the 2-dialkyl-1,3-dicyclohexylguanidinate, it is useful to also define a Δ'_{CN} value, determined as the difference between the average value of the C–N$_{\text{amidine}}$ bond length and the C–N$_{\text{amide}}$ distance.[64] A positive Δ'_{CN} value would indicate contribution from a resonance form where the maximum negative charge is located on the coordinating N-donors. The calculated Δ'_{CN} values for complexes **1**–**8** are all negative, ranging from −0.0405 Å in **7** to −0.106 Å in **5**. The negative value indicates a small degree of zwitterionic resonance, and is consistent with guanidinate coordination to metals with small coordination spheres (Li) and to electron-rich metals (Cu, Ag, and Au). Overall, there was no distinct trend in the negative Δ'_{CN} values that could be attributed to the different metal or NR$_2$ substituent.

DFT Calculations

To investigate any possible d^{10}–d^{10} metallophilic interactions, a theoretical inquiry (Fig. S5) of {Cu[CyNC(NEt$_2$)NCy]}$_2$ (**4**) and {Ag[CyNC(NEt$_2$)NCy]}$_3$ (**6**) was performed.[38] Using the atom coordinates for **4** and **6** garnered from the single crystal X-ray diffraction investigation, the molecular orbitals for **4** and **6** were calculated at the B3 LYP/LANL2DZ[33–36] level of theory. The orbitals are depicted in Fig. S5 (Supplementary Material). For each structure, localized d-atomic orbitals (AOs), instead of delocalized electron density between the metal atoms, are observed, suggesting negligible M–M interaction. To further evaluate the bonding, the natural bond orbital (NBO) analysis[37,39,40] at the B3 LYP/LANL2DZ[33–36] level of theory was performed for **4** and **6**.

According to the NBO analysis, the Cu atoms in **4** have $4s^{0.7}3d^{9.5}$ valence atomic occupations and an effective atomic charge of +0.72 e, whereas the coordinating N atoms each have $2s^{1.4}2p^{4.4}$ atomic occupation and an effective atomic charge of −0.79 e. Each Cu–N bond showed an average of 89 % nitrogen character (25 % s-character and 75 % p-character) and 11 % copper character (78 % s-character and 22 % p-character). The hybridization for each Cu–N bond is $0.33(sd^{0.3})\text{Cu} + 0.95(sp^{3.0})\text{N}$, displaying the expected sp^3 hybridization on the N atoms. These results are analogous to those found for the copper dimer, Cu$_2$(hpp)$_2$ (hpp [L^2] = 1,3,4,6,7,8-hexahydro-2H-pyrimido[1,2-a]pyrimidinato), in which the NBO analysis exhibited a $4s^{0.6}3d^{9.8}$ configuration for the Cu atoms, indicating that the Cu atoms have nearly occupied 3d-AOs and are partially reduced by the electron donating effect of the N atom.[58]

For complex **6,** the three Ag atoms have an average of $5s^{0.53}4d^{9.82}$ valence atomic occupation and an effective atomic charge of +0.63 e, and the N atoms have $2s^{1.312}p^{4.38}$ atomic occupations and an effective atomic charge of −0.73 e. Examination of the atomic occupation of Ag indicates that the 4d-AOs are almost completely occupied and thus the net bonding effect from molecular orbitals (MOs) composed of 4d-AOs is not significant. The average hybridization for each Ag–N bond shows $0.31(sd^{0.10})$ Ag + $0.95(sp^{3.51})$N, exhibiting sp^3 hybridization of the N atoms. Each Ag–N bond showed an average of 90 % N character (22 % s-character and 78 % p-character), with the difference being Ag character (90 % s-character and 10 % p-character).

Overall, the results of the NBO analysis are consistent with the calculated molecular orbitals. The short Cu and Ag inter-atomic distances are attributed to the coordination of the guanidinate ligands and not due to significant M–M interactions. Furthermore, the results and conclusions drawn for the Cu bonding in **4** are consistent with studies conducted on the structurally and electronically similar Cu guanidinate complex, $[Cu_2(hpp)_2]$.[58]

Conclusion

Overall, in this work, 2,2-dialkyl-1,3-dicyclohexylguanidinate was shown to be a useful ligand for the isolation of a family of eight Li, Cu, Ag, and Au guanidinate complexes. This synthetic and structural investigation contributes to the growing field of L^1-type guanidinate chemistry and further adds to the limited number of examples of stable Lewis base-free complexes containing Group 11 nitrogen bonds. Altering the steric bulk of the dialkyl group (NMe_2 versus NEt_2) did not alter the nuclearity of the Cu, Ag, and Au systems. However, the diakyl group does have an effect on the resulting M–N and M–M inter-atomic distances; for the Cu and Au systems, the NEt_2 substituent was found to generate compounds with shorter M–N and M–M inter-atomic distances. Theoretical investigations of the Cu and Ag systems indicate a negligible M–M bonding contribution to the short inter-atomic distances. The synthesis of additional guanidinate clusters is currently under investigation.

Supplementary Material

Plots for **2**, **3**, **6**, and **8**, molecular orbital diagrams and Cartesian coordinates are available on the Journal's website. Crystallographic data for the structures have been deposited with the Cambridge Crystallographic Data Centre as supplementary publication Nos. CCDC 988466 for **1**, CCDC 988467 for **2**, CCDC 988468 for **3**, CCDC 988469 for **4**, CCDC 988470 for **5**, CCDC 988471 for **6**, CCDC 988472 for **7**, and CCDC 988644 for **8**. Copies of the data can be obtained on application to CCDC, 12 Union Road, Cambridge CB2 1EZ, UK; fax: +44(0) 1223 336 033; email: deposit@ccdc.cam.ac.uk.

Acknowledgements

The authors acknowledge Kent State University and the National Science Foundation through the Ohio Consortium for Undergraduate Research: Research Experiences to Enhance Learning (REEL) Award No. 0532250.

References

[1] I. Pattison, K. Wade, B. K. Wyatt, *J. Chem. Soc. A* **1968**, 837. doi:10.1039/J19680000837

[2] W. Schneider, A. Bauer, A. Schier, H. Schmidbaur, *Chem. Ber.* **1997**, *130*, 1417. doi:10.1002/CBER.19971301010

[3] N. Kuhn, R. Fawzi, M. Steimann, J. Wiethoff, *Z. Anorg. Allg. Chem.* **1997**, *623*, 554. doi:10.1002/ZAAC.19976230186

[4] N. De Vries, C. E. Costello, A. G. Jones, A. Davison, *Inorg. Chem.* **1990**, *29*, 1348. doi:10.1021/IC00332A012

[5] M. A. Paver, D. S. Wright, D. Stalke, *Angew. Chem. Int. Ed. Engl.* **1993**, *32*, 428. doi:10.1002/ANIE.199304281

[6] W. Clegg, R. Snaith, H. M. M. Shearer, K. Wade, G. Whitehead, *J. Chem. Soc., Dalton Trans.* **1983**, 1309. doi:10.1039/DT9830001309

[7] W. Clegg, R. E. Mulvey, R. Snaith, G. E. Toogood, K. Wade, *J. Chem. Soc. Chem. Commun.* **1986**, 1740. doi:10.1039/C39860001740

[8] A. J. Edwards, M. A. Paver, P. R. Raithby, M.-A. Rennie, C. A. Russell, D. S. Wright, *J. Chem. Soc., Dalton Trans.* **1995**, 1587. doi:10.1039/DT9950001587

[9] R. Longhi, R. S. Drago, *Inorg. Chem.* **1965**, *4*, 11. doi:10.1021/IC50023A002

[10] P. J. Bailey, S. Pace, *Coord. Chem. Rev.* **2001**, *214*, 91. doi:10.1016/S0010-8545(00)00389-1

[11] A. R. Cowley, A. J. Downs, H. J. Himmel, S. Marchant, S. Parsons, J. A. Yeoman, *Dalton Trans.* **2005**, 1591. doi:10.1039/B501818H

[12] M. P. Coles, *Dalton Trans.* **2006**, 985. doi:10.1039/B515490A

[13] F. T. Edelmann, in *Recent Progress in the Chemistry of Metal Amidinates, Guanidinates: Syntheses, Catalysis, Materials* (Eds A. F. Hill, M. J. Fink) **2013**, Vol. 61, pp. 55–374 (Elsevier Academic Press Inc: San Diego, CA).

[14] M. P. Coles, *Chem. Commun.* **2009**, 3659. doi:10.1039/B901940E

[15] F. T. Edelmann, in *Advances in the Coordination Chemistry of Amidinate, Guanidinate Ligands* (Eds A. F. Hill, M. J. Fink) **2008**, Vol. 57, p. 183–352 (Elsevier Academic Press Inc: San Diego, CA).

[16] A. Gobbi, G. Frenking, *J. Am. Chem. Soc.* **1993**, *115*, 2362. doi:10.1021/JA00059A035

[17] R. Kempe, *Angew. Chem. Int. Ed.* **2000**, *39*, 468. doi:10.1002/(SICI)1521-3773(20000204)39:3<468::AID-ANIE468>3.0.CO;2-G

[18] T. J. J. Whitehorne, J. P. Coyle, A. Mahmood, W. H. Monillas, G. P. A. Yap, S. T. Barry, *Eur. J. Inorg. Chem.* **2011**, 3240. doi:10.1002/EJIC.201100262

[19] T. Kim, Y. Yao, J. P. Coyle, S. T. Barry, F. Zaera, *Chem. Mater.* **2013**, *25*, 3630. doi:10.1021/CM401707H

[20] M. D. Irwin, H. E. Abdou, A. A. Mohamed, J. P. Fackler, *Chem. Commun.* **2003**, 2882. doi:10.1039/B309724M

[21] H. E. Abdou, A. A. Mohamed, J. P. Fackler, *Inorg. Chem.* **2007**, *46*, 141. doi:10.1021/IC0612449

[22] A. A. Mohamed, A. P. Mayer, H. E. Abdou, M. D. Irwin, L. M. Perez, J. P. Fackler, *Inorg. Chem.* **2007**, *46*, 11165. doi:10.1021/IC701399S

[23] A. A. Mohamed, H. E. Abdou, A. Mayer, J. P. Fackler, *J. Clust. Sci.* **2008**, *19*, 551. doi:10.1007/S10876-008-0198-1

[24] J. P. Coyle, P. A. Johnson, G. A. DiLabio, S. T. Barry, J. Müller, *Inorg. Chem.* **2010**, *49*, 2844. doi:10.1021/IC902247W

[25] J. A. Bertke, S. D. Bunge, *Dalton Trans.* **2007**, 4647. doi:10.1039/B712054K

[26] S. D. Bunge, J. M. Lance, J. A. Bertke, *Organometallics* **2007**, *26*, 6320. doi:10.1021/OM700501G

[27] T. L. Cleland, S. D. Bunge, *Polyhedron* **2007**, *26*, 5506. doi:10.1016/J.POLY.2007.08.013

[28] S. D. Bunge, J. A. Bertke, T. L. Cleland, *Inorg. Chem.* **2009**, *48*, 8037. doi:10.1021/IC9007153

[29] S. D. Bunge, J. A. Ocana, T. L. Cleland, J. L. Steele, *Inorg. Chem.* **2009**, *48*, 4619. doi:10.1021/IC9003627

[30] T. E. Janini, R. Rakosi, C. B. Durr, J. A. Bertke, S. D. Bunge, *Dalton Trans.* **2009**, 10601. doi:10.1039/B917377C

[31] J. D. Monegan, S. D. Bunge, *Inorg. Chem.* **2009**, *48*, 3248. doi:10.1021/IC8022776

[32] A. M. Willcocks, T. P. Robinson, C. Roche, T. Pugh, S. P. Richards, A. J. Kingsley, J. P. Lowe, A. L. Johnson, *Inorg. Chem.* **2012**, *51*, 246. doi:10.1021/IC201602M

[33] A. D. Becke, *J. Chem. Phys.* **1993**, *98*, 5648. doi:10.1063/1.464913

[34] C. Lee, W. Yang, R. G. Parr, *Phys. Rev.* **1998**, *B37*, 785.

[35] A. J. H. Wachters, *J. Chem. Phys.* **1970**, *52*, 1033. doi:10.1063/1.1673095
[36] P. J. Hay, *J. Chem. Phys.* **1977**, *66*, 4377. doi:10.1063/1.433731
[37] A. E. Reed, R. B. Weinstock, F. Weinhold, *J. Chem. Phys.* **1985**, *83*, 735. doi:10.1063/1.449486
[38] *Spartan '04 for Windows* **2004** (Wavefunction, Inc.: Irvine, CA).
[39] M. J. Frisch, G. W. Trucks, H. B. Schlegel, G. E. Scuseria, M. A. Robb, J. R. Cheeseman, V. G. Zakrzewski, J. A. Montgomery, R. E. Stratmann, J. C. Burant, S. Dapprich, J. M. Millam, A. D. Daniels, K. N. Kudin, M. C. Strain, O. Farkas, J. Tomasi, V. Barone, M. Cossi, R. Cammi, B. Mennucci, C. Pomelli, C. Adamo, S. Clifford, J. Ochterski, G. A. Petersson, P. Y. Ayala, Q. Cui, K. Morokuma, D. K. Malick, A. D. Rabuck, K. Raghavachari, J. B. Foresman, J. Cioslowski, J. V. Ortiz, B. B. Stefanov, G. Liu, A. Liashenko, P. Piskorz, I. Komaromi, R. Gomperts, R. L. Martin, D. J. Fox, T. Keith, M. A. Al-Laham, C. Y. Peng, A. Nanayakkara, C. Gonzalez, M. Challacombe, P. M. W. Gill, B. Johnson, W. Chen, M. W. Wong, J. L. Andres, C. Gonzalez, M. Head-Gordon, E. S. Replogle, J. A. Pople, *Gaussian 98, Revision A.11.2* **2001** (Gaussian, Inc.: Pittsburgh, PA).
[40] E. D. Glendening, A. E. Reed, J. E. Carpenter, F. Weinhold, *NBO Version 3.1* **1996** (Theoretical Chemistry Institute, University of Wisconsin: Madison, WI)
[41] H. Shen, H. S. Chan, Z. W. Xie, *Organometallics* **2006**, *25*, 5515. doi:10.1021/OM060811X
[42] M. K. T. Tin, G. P. A. Yap, D. S. Richeson, *Inorg. Chem.* **1999**, *38*, 998. doi:10.1021/IC980709V
[43] A. Baunemann, M. Winter, K. Csapek, C. Gemel, R. A. Fischer, *Eur. J. Inorg. Chem.* **2006**, 4665. doi:10.1002/EJIC.200600653
[44] H. Hao, C. Cui, G. Bai, H. W. Roesky, M. Noltemeyer, H.-G. Schmidt, Y. Ding, *Z. Anorg. Allg. Chem.* **2000**, *626*, 1660. doi:10.1002/1521-3749(200007)626:7<1660::AID-ZAAC1660>3.0.CO;2-J
[45] X.-A. Pang, Y.-M. Yao, J.-F. Wang, H.-T. Sheng, Y. Zhang, Q. Shen, *Chin. J. Chem.* **2005**, *23*, 1193. doi:10.1002/CJOC.200591193
[46] Y. Zhang, M. Wang, Y. Yao, Q. Shen, *Chin. Sci. Bull.* **2005**, *50*, 2817.
[47] H. Shen, H.-S. Chan, Z. Xie, *J. Am. Chem. Soc.* **2007**, *129*, 12934. doi:10.1021/JA0754498
[48] J.-F. Sun, X.-T. Chen, Z.-L. Xue, *Inorg. Chim. Acta* **2009**, *362*, 4251. doi:10.1016/J.ICA.2009.05.049
[49] T. K. Panda, H. Tsurugi, K. Pal, H. Kaneko, K. Mashima, *Organometallics* **2010**, *29*, 34. doi:10.1021/OM901027V
[50] B. Sharma, S.-J. Chen, J. K. C. Abbott, X.-T. Chen, Z.-L. Xue, *Inorg. Chem.* **2012**, *51*, 25. doi:10.1021/IC2021676
[51] G. R. Giesbrecht, A. Shafir, J. Arnold, *J. Chem. Soc., Dalton Trans.* **1999**, 3601. doi:10.1039/A904295D
[52] D. Rudolf, E. Kaifer, H. J. Himmel, *Eur. J. Inorg. Chem.* **2010**, 4952. doi:10.1002/EJIC.201000598
[53] H. F. Han, W. J. Li, H. Y. Li, *Acta Crystallogr. E* **2010**, *E66*, m1579. doi:10.1107/S1600536810046477
[54] X. A. Pang, Y. M. Yao, J. F. Wang, H. T. Sheng, Y. Zhang, Q. Shen, *Chin. J. Chem.* **2005**, *23*, 1193. doi:10.1002/CJOC.200591193
[55] C. L. Boyd, B. R. Tyrrell, P. Mountford, *Acta Crystallogr. E* **2002**, *E58*, m597. doi:10.1107/S1600536802017579
[56] C. F. Caro, P. B. Hitchcock, M. F. Lappert, M. Layh, *Chem. Commun.* **1998**, *12*, 1297. doi:10.1039/A708976G
[57] L. Yang, D. R. Powell, R. P. Houser, *Dalton Trans.* **2007**, 955. doi:10.1039/B617136B
[58] F. A. Cotton, X. J. Feng, D. J. Timmons, *Inorg. Chem.* **1998**, *37*, 4066. doi:10.1021/IC980137E
[59] F. A. Cotton, G. Wilkinson, C. A. Murillo, M. Bochmann, *Advances in Inorganic Chemistry* **1999** (Wiley-Interscience: New York, NY).
[60] B. S. Lim, A. Rahtu, J. S. Park, R. G. Gordon, *Inorg. Chem.* **2003**, *42*, 7951. doi:10.1021/IC0345424
[61] J. P. Coyle, W. H. Monillas, G. P. A. Yap, S. T. Barry, *Inorg. Chem.* **2008**, *47*, 683. doi:10.1021/IC701317Y
[62] Z. W. Li, S. T. Barry, R. G. Gordon, *Inorg. Chem.* **2005**, *44*, 1728. doi:10.1021/IC048492U
[63] S. Patai, Z. Rappoport, *The Chemistry of Amidines and Imidinates* (*2*) **1991** (Wiley: New York, NY).
[64] M. P. Coles, P. B. Hitchcock, *Organometallics* **2003**, *22*, 5201. doi:10.1021/OM0341092
[65] C. Jones, C. Schulten, L. Fohlmeister, A. Stasch, K. S. Murray, B. Moubaraki, S. Kohl, M. Z. Ertem, L. Gagliardi, C. J. Cramer, *Chem. Eur. J.* **2011**, *17*, 1294. doi:10.1002/CHEM.201002388